J. Fluid Mech. (2019), *vol.* 864, *pp.* 73–96.
doi:10.1017/jfm.2018.1011

Forced synchronization and asynchronous quenching of periodic oscillations in a thermoacoustic system

Sirshendu Mondal[1,†], **Samadhan A. Pawar**[1] **and R. I. Sujith**[1]

[1]Department of Aerospace Engineering, Indian Institute of Technology Madras, Chennai 600036, India

(Received 18 May 2018; revised 25 October 2018; accepted 5 December 2018;
first published online 1 February 2019)

We perform an experimental and theoretical study to investigate the interaction between an external harmonic excitation and a self-excited oscillatory mode (f_{n0}) of a prototypical thermoacoustic system, a horizontal Rijke tube. Such an interaction can lead to forced synchronization through the routes of phase locking or suppression. We characterize the transition in the synchronization behaviour of the forcing and the response signals of the acoustic pressure while the forcing parameters, i.e. amplitude (A_f) and frequency (f_f) of forcing are independently varied. Further, suppression is categorized into synchronous quenching and asynchronous quenching depending upon the value of frequency detuning ($|f_{n0} - f_f|$). When the applied forcing frequency is close to the natural frequency of the system, the suppression in the amplitude of the self-excited oscillation is known as synchronous quenching. However, this suppression is associated with resonant amplification of the forcing signal, leading to an overall increase in the response amplitude of oscillations. On the other hand, an almost 80 % reduction in the root mean square value of the response oscillation is observed when the system is forced for a sufficiently large value of the frequency detuning (only for $f_f < f_{n0}$). Such a reduction in amplitude occurs due to asynchronous quenching where resonant amplification of the forcing signal does not occur, as the frequency detuning is significantly high. Further, the results from a reduced-order model developed for a horizontal Rijke tube show a qualitative agreement with the dynamics observed in experiments. The relative phase between the acoustic pressure (p') and the heat release rate ($\dot{q}'$) oscillations in the model explains the occurrence of maximum reduction in the pressure amplitude due to asynchronous quenching. Such a reduction occurs when the positive coupling between p' and $\dot{q}'$ is disrupted and their interaction results in overall acoustic damping, although both of them oscillate at the forcing frequency. Our study on the phenomenon of asynchronous quenching thus presents new possibilities to suppress self-sustained oscillations in fluid systems in general.

Key words: instability control, noise control, nonlinear instability

† Present address: Department of Mechanical Engineering, National Institute of Technology, Durgapur 713209, India. Email address for correspondence: sirshendumondal13@gmail.com

1. Introduction

Self-sustained oscillations occur due to hydrodynamic instabilities observed in the wakes behind bluff bodies (Provansal, Mathis & Boyer 1987; Monkewitz 1988; Emerson *et al.* 2012), and in the flow field of low density jets (Huerre & Monkewitz 1985; Li & Juniper 2013*a*) and are also due to thermoacoustic interactions in confined reacting flows (Crocco & Cheng 1956; Oyediran, Darling & Radhakrishnan 1995; Lieuwen & Yang 2005). Systems having temporally unstable global modes behave as oscillators (Huerre & Monkewitz 1990). Harmonic excitation of such unstable mean flows essentially modulates the generation of large-scale coherent structures, thereby enhancing the transport of momentum across the flow (Greenblatt & Wygnanski 2000). Therefore, efficient mixing through high momentum transfer and control of intrinsic global modes can be achieved through a rigorous understanding of the interaction between the external excitation and the intrinsic oscillatory modes observed in fluid mechanical systems. In the present study, we investigate this interaction in a thermoacoustically unstable system where an external harmonic forcing is used to suppress unwanted self-sustained periodic oscillations.

Thermoacoustic instability has hampered the development of practical combustion systems such as gas turbine engines, rocket motors and industrial burners (Juniper & Sujith 2018). Such an instability refers to the occurrence of large amplitude pressure oscillations in a combustion chamber. These instabilities occur primarily due to a closed loop interaction between the acoustic waves (p') inside the combustor and the unsteady heat release rate ($\dot{q}'$) from the flame. Large levels of vibration caused due to thermoacoustic instability can lead to catastrophic consequences such as structural damage or reduction in the lifetime of combustors (Sujith, Juniper & Schmid 2016). Therefore, there is a need to either control such instabilities or to suppress them completely.

Various methods have been devised over the years to control these instabilities and thereby increase the operational range of the engines (Dowling & Morgans 2005). The control strategies used in the past to suppress thermoacoustic instabilities are of different kinds. Open-loop control strategies, which were able to reduce the thermoacoustic coupling between the acoustic field and the unsteady heat release rate, include perturbing either the shear layers in the flow field (McManus, Vandsburger & Bowman 1990) or the acoustic field of the combustor (Najm & Ghoniem 1991). Closed-loop control has also been implemented in a Rijke tube (Dines 1984; Heckl 1988), ducted premixed flame (Lang, Poinsot & Candel 1987*b*) and in a turbulent diffusion flame (Lang *et al.* 1987*a*) to suppress the amplitude of acoustic pressure oscillations through the mechanism of negative feedback between the self-excited sound waves, and the imposed sound waves (external acoustic perturbations). Note that in open-loop control, forcing is applied at different frequencies other than the natural frequency, whereas, in closed-loop control, the feedback signal is applied at the natural frequency, but is phase shifted (Lubarsky *et al.* 2003).

1.1. *Forcing on self-sustained oscillatory systems including reacting flow systems*

Harmonic forcing has also found its application in self-sustained oscillatory systems. Lubarsky *et al.* (2003) experimentally studied the effect of fuel flow modulation at a non-resonant frequency on the self-excited thermoacoustic oscillations in a swirl-stabilized combustor. Bellows, Neumeier & Lieuwen (2006) studied the nonlinear response of the heat release rate fluctuations to flow perturbations in the context of a swirling premixed flame. The response in the heat release rate oscillation was shown

to saturate at a sufficiently high amplitude of forcing. In a different study, Bellows, Hreiz & Lieuwen (2008) reported the effectiveness of forcing for controlling the self-excited thermoacoustic oscillations. However, they observed a reduction in amplitude only for a few selected forcing frequencies. Therefore, a systematic investigation of forced response for a wide range of forcing frequency and amplitude is desirable in a thermoacoustic system to qualitatively identify the regime of amplitude reduction in terms of the forcing parameters. Further, characterizing the dynamical states and mechanisms of amplitude reduction in the context of dynamical systems theory is essential for a better understanding of the phenomenon. In a recent study by Kashinath, Li & Juniper (2018), forced synchronization leading to periodic, quasi-periodic and chaotic states is investigated quite elaborately using a simple model of a ducted laminar flame; however, experimental realization of this study is still limited.

Further, upon the application of harmonic excitation on hydrodynamically self-excited flames, different kinds of dynamics and bifurcations have been observed (Li & Juniper 2013*b*) before an eventual phase locking between the forcing signal and the natural oscillations of the system. In the recent past, the effect of external acoustic forcing has been investigated elaborately in self-excited jets (Li & Juniper 2013*a*,*c*) and self-excited flames (Li & Juniper 2013*b*). They have reported different dynamical states including quasiperiodicity (Li & Juniper 2013*a*,*b*) as well as different synchronization states including phase slipping and phase trapping (Li & Juniper 2013*c*). Further, Hochgreb and her co-workers (Kim & Hochgreb 2011, 2012; Balusamy *et al.* 2015; Han, Balusamy & Hochgreb 2015; Han & Hochgreb 2015; Balusamy *et al.* 2017) have extensively studied the dynamics and the response of stratified lean-premixed flames subjected to external acoustic velocity perturbations. Most of their studies (Kim & Hochgreb 2011, 2012; Han *et al.* 2015; Han & Hochgreb 2015; Balusamy *et al.* 2017) were focussed on investigating the forced flame response by estimating the flame transfer/describing functions (FTF/FDF). Balusamy *et al.* (2015), however, characterized the forced dynamics of a self-excited thermoacoustic system using the framework of forced synchronization. They reported the observations of pulling or pushing of the response frequency associated with the self-excited mode towards or away from the forcing frequency for different conditions of harmonic forcing.

Yoshida *et al.* (2013) investigated forced synchronization phenomena in a thermoacoustic engine, wherein the pressure oscillations are amplified and sustained due to the temperature gradient between heat exchangers and not due to the unsteady heat release rate from the flame. They have evidenced the reduction in amplitude associated with the natural dynamics for a selected value of frequency detuning. Although some progress has been made in understanding the response dynamics of forced limit cycle oscillations of thermoacoustic systems, the reduction in the overall response amplitude (amplitude of the forced system) due to forcing needs more rigorous investigation.

In the present study, we experimentally and theoretically investigate the effect of forcing on the self-excited periodic oscillations developed in a thermoacoustic system, the horizontal Rijke tube. We further show a qualitative similarity of the forced dynamics observed in the experiments with a reduced-order model developed for the system. One of the objectives is to obtain a complete picture in terms of response dynamics as well as synchronization behaviour of the forced thermoacoustic system.

1.2. *Forced synchronization and amplitude quenching*

The phenomenon of forced synchronization (synchronization of unidirectionally coupled periodic oscillators) has been gaining increased attention and has been

extensively studied both theoretically (Pikovsky, Rosenblum & Kurths 2003; Balanov *et al.* 2009) and experimentally (Kiss & Hudson 2001; Boccaletti *et al.* 2002; Battogtokh, Aihara & Tyson 2006). The forced response of a system depends on the values of the frequency and the amplitude of forcing. Such response dynamics of a forced system can be effectively represented by a synchronization region in the parametric space of forcing amplitude and frequency, known as the Arnold tongue (Balanov *et al.* 2009). Most of the theoretical studies on forced synchronization are based on van der Pol oscillators, which mimic a variety of oscillatory phenomena in electric circuits (van der Pol 1920), electrocardiograms (Van Der Pol & Van Der Mark 1928), semiconductor lasers (Blažek 1968), neuronal activity (Nomura *et al.* 1993), etc. Further, the phenomenon of forced synchronization has been experimentally implemented to control or suppress chaos (Anishchenko *et al.* 1992; Kiss & Hudson 2001), and also to suppress oscillatory instability (Keen & Fletcher 1969). Using a simple experimental set-up consisting of an organ pipe and a loudspeaker, Abel, Ahnert & Bergweiler (2009) gave an experimental evidence of forced synchronization in acoustics.

Forced synchronization of periodic oscillations is usually achieved through the routes of phase locking and suppression (Balanov *et al.* 2009). Upon increasing the forcing amplitude, when the frequency difference between the forcing and the natural oscillation of a given system is very small, the frequency of forced oscillations, also called the main frequency in other literature (Balanov *et al.* 2009), shifts gradually towards the forcing frequency (f_f) and, finally, coincides with f_f; the mechanism is known as phase locking. Hereafter, we call the frequency of forced oscillation the response frequency (f_r). On the other hand, suppression of the self-sustained oscillations occurs for a relatively larger value of the frequency difference, wherein the amplitude of natural oscillations is suppressed without exhibiting any shift in frequency, as the forcing amplitude is increased. The route of phase locking is attained through a saddle-node bifurcation, whereas, the suppression route is reached through a torus-death bifurcation (Balanov *et al.* 2009; Hyodo & Biwa 2018).

Suppression is further classified as synchronous quenching (Odajima, Nishida & Hatta 1974; Ohsawa 1980) and asynchronous quenching (Minorsky 1967) depending upon the value of frequency detuning between the forcing and the natural oscillation. When the frequency detuning is relatively small, the suppression of self-sustained oscillation is known as synchronous quenching. However, synchronous quenching of natural oscillation is associated with resonance amplification of the forcing signal, in which the overall response amplitude of the forced system increases to a higher value in the synchronization region. On the other hand, when frequency detuning is relatively large, the suppression of self-sustained oscillation is known as asynchronous quenching (Minorsky 1967) where the resonant amplification of the forcing signal does not occur. Such a type of suppression is caused by an asymptotic loss of stability of self-excited oscillations due to the disturbance induced by the imposed forcing and leads to a reduction in the overall amplitude of the forced system (Keen & Fletcher 1969).

Therefore, studying the applicability of asynchronous quenching is important to mitigate the amplitude of undesired acoustic oscillations observed in practical combustors. Such a type of suppression phenomenon was experimentally evidenced in the control of ion-sound instability (Keen & Fletcher 1969), in self-excited ionization waves (Ohe & Takeda 1974) and even in the control of thermoacoustic instability (Guan *et al.* 2018). Further, the reduction in response amplitude of thermoacoustic oscillation forced at non-resonant frequencies has been reported in previous studies

(Lubarsky *et al.* 2003; Bellows *et al.* 2008; Guan *et al.* 2018; Kashinath *et al.* 2018). However, they did not focus on explaining the mechanism behind such a quenching of natural oscillations due to forcing. In the present study, we apply the knowledge of forced synchronization and the associated quenching phenomena in studying systematically the forced response of limit cycle oscillations of a horizontal Rijke tube.

We employ external harmonic forcing through a system of acoustic drivers when the system dynamics exhibits self-sustained limit cycle oscillations at the fundamental longitudinal mode of the duct. By varying the amplitude and frequency (across the natural frequency) of forcing, we report an experimental observation of synchronous quenching of self-sustained oscillation and resonant amplification of the forcing in the synchronization region of the Arnold tongue along with the exhibition of different states during the process of forced synchronization. We, further, report an experimental observation of a significant reduction in root-mean-square (r.m.s.) amplitude of natural oscillations (by 80 % of the unforced value) when the system is forced with a frequency far lower than the natural frequency (in the present case, it happens to be close to a subharmonic frequency). We also observe qualitatively similar dynamics in a theoretical model developed for the horizontal Rijke tube (Balasubramanian & Sujith 2008). By varying the forcing amplitude and the forcing frequency, we explore the phenomena of synchronous and asynchronous quenching in the model. We further try to explore the effect of harmonic forcing on the thermoacoustic coupling between the acoustic pressure (p') and the heat release rate ($\dot{q}'$) oscillations obtained from the model. The phenomenon of asynchronous quenching is found to be associated with a shift in phase difference between p' and $\dot{q}'$ from zero (during phase synchronization) to $\pi/2$.

2. Experimental set-up

We perform experiments on a horizontal Rijke tube (schematic shown in figure 1), which is 1 m long with a square cross-section (9.2 cm $\times$ 9.2 cm). An electrically heated wire mesh acts as a compact heat source which is powered by an external DC power supply. The mean flow of air is provided by means of a compressor and is maintained constant at 100 slpm using a mass flow controller (Alicat Scientific, MCR series, with an uncertainty of $\pm$(0.8 % of the reading + 0.2 % of full scale) and the range of 0–500 slpm). The air is passed through a rectangular chamber (120 cm $\times$ 45 cm $\times$ 45 cm), referred to as a decoupler, to eliminate the upstream fluctuations (hydrodynamic and acoustic) and to make the inlet flow steady. Therefore, pressure fluctuations at both ends of the Rijke tube become negligible. A detailed description of the set-up can be found in Gopalakrishnan & Sujith (2015).

The location of the heater inside the duct is held constant throughout the study at 27 cm from the end connected to the decoupler. Four wall mounted acoustic drivers (loud speaker, Ahuja AU60, at a distance of 62.5 cm from the inlet) along with an amplifier are used to provide harmonic forcing signal in the system. Note that the forcing amplitude of the loudspeaker is expressed in its input unit, i.e. mV, throughout the paper and not converted into physical units such as that of acoustic velocity (m s^{-1}) or pressure amplitude (Pa). Such conversions can be done through several means (Li & Juniper 2013*a*; Balusamy *et al.* 2015). We retain the mV readings, considering the fact that such peak-to-peak voltage is directly proportional to the amplitude of acoustic pressure (Li & Juniper 2013*a*).

A piezoelectric transducer (PCB 103B02, sensitivity 217.5 mV kPa^{-1} and uncertainty $\pm$0.15 Pa) mounted at the wall, close to the midpoint along the length of the

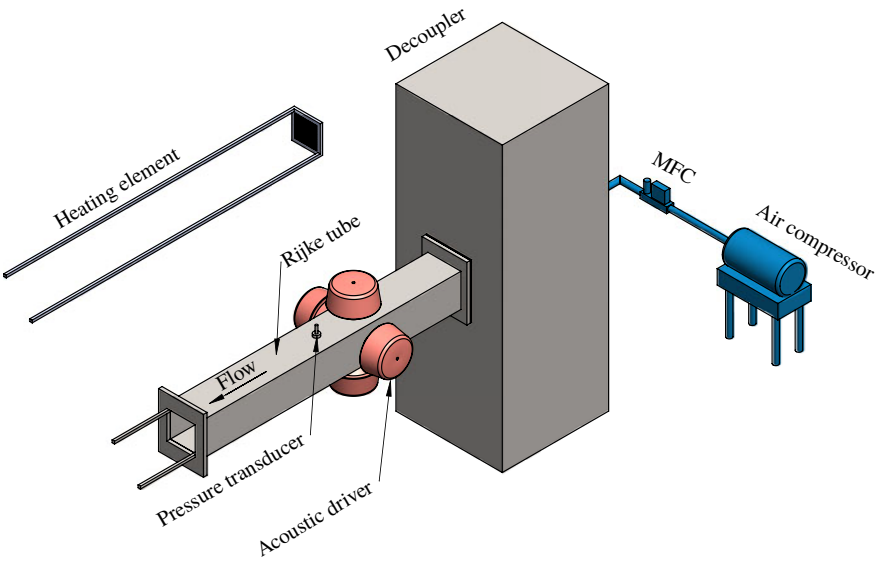

FIGURE 1. (Colour online) Schematic of a horizontal Rijke tube set-up used in the present study.

duct, is used to measure the acoustic pressure fluctuations in the system. The system is preheated for 10 min by supplying a constant voltage of 3.5 V to the heater to ensure that the temperature is steady in the vicinity of the heater. The subcritical Hopf bifurcation takes place at a heater power value of 1.21 kW (uncertainty ± 0.4 W). For the forcing study, the power supplied to the heater is maintained constant at 1.24 kW throughout the experiments. Data are acquired at a sampling frequency of 10 kHz. The bin size (frequency resolution) of the fast Fourier transform of the measured signal is 0.3 Hz. To ensure consistent ambient conditions, we maintain an initial temperature at $23 \pm 3\,^{\circ}\mathrm{C}$ and a relative humidity at 55 % for each experiment. We also determine the exponential decay rate of the system by giving an acoustic pulse in the absence of the flow (Mariappan 2012). To ensure repeatability, the experiments are conducted only when the decay rate lies within $\pm 10\,\%$ of the mean value, found to be 19.0 s^{-1}.

3. Model

We use a reduced-order model for the horizontal Rijke tube developed by Balasubramanian & Sujith (2008). The model for a one-dimensional acoustic field is derived from the linearized momentum (3.1) and energy (3.2) equations for a medium with a perfect, inviscid and non-heat-conducting gas, neglecting the effects of mean flow (zero Mach number approximation, Nicoud & Wieczorek 2009) and mean temperature gradient:

$$\bar{\rho}\frac{\partial \tilde{u}'}{\partial \tilde{t}} + \frac{\partial \tilde{p}'}{\partial \tilde{x}} = 0, \tag{3.1}$$

$$\frac{\partial \tilde{p}'}{\partial \tilde{t}} + \gamma \bar{p}\frac{\partial \tilde{u}'}{\partial \tilde{x}} = (\gamma - 1)\dot{\tilde{Q}}'\delta(\tilde{x} - \tilde{x}_f), \tag{3.2}$$

where ρ and γ are the density and the ratio of specific heats of the medium. The heat release rate ($\dot{\tilde{Q}}'$) in the duct is modelled using a modified form of King's law (King

1914) given by Heckl (1990). The variables are non-dimensionalized and the resulting set of partial differential equations is then reduced to a set of ordinary differential equations (ODE) using the Galerkin technique (Lores & Zinn 1973). To that end, the non-dimensional velocity (u') and the non-dimensional pressure (p') fluctuations in the duct are written in terms of basis functions or the Galerkin modes (Balasubramanian & Sujith 2008). These basis functions are essentially the natural acoustic modes of the duct in the absence of heat release. These functions further satisfy the boundary conditions $[p'(0, t) = 0;\ p'(1, t) = 0]$ and can be written as follows:

$$u'(x, t) = \sum_{j=1}^{N} \eta_j(t) \cos(j\pi x), \tag{3.3}$$

$$p'(x, t) = -\sum_{j=1}^{N} \dot{\eta}_j(t) \frac{\gamma M}{j\pi} \sin(j\pi x), \tag{3.4}$$

where η_j and $\dot{\eta}_j$ represent the time varying coefficients of the jth mode of the acoustic velocity (u') and the acoustic pressure (p'), respectively, and N represents the number of Galerkin modes considered. Here, M is the Mach number of the mean flow and γ is the ratio of specific heats of air at ambient condition.

The temporal evolution of the system is thus described by the following set of ordinary differential equations:

$$\frac{\mathrm{d}\eta_j}{\mathrm{d}t} = \dot{\eta}_j, \tag{3.5}$$

$$\frac{\mathrm{d}\dot{\eta}_j}{\mathrm{d}t} + 2\zeta_j\omega_j\dot{\eta}_j + {\omega_j}^2\eta_j = -j\pi K \left[\sqrt{\left|\frac{1}{3} + u'_f(t-\tau)\right|} - \sqrt{\frac{1}{3}}\right] \sin(j\pi x_f), \tag{3.6}$$

where

$$u'_f(t-\tau) = \sum_{j=1}^{N} \eta_j(t-\tau) \cos(j\pi x_f). \tag{3.7}$$

Other parameters are the damping coefficient of the jth mode, ζ_j, non-dimensional angular frequency, ω, non-dimensional heater power, K, and non-dimensional velocity, u'_f at the non-dimensional heater location, x_f. Variables with a tilde are dimensional and those without a tilde are non-dimensional. Here, K is analogous to the heater power in experiments and ζ_j is frequency-dependent damping (Sterling & Zukoski 1991) given by

$$\zeta_j = \frac{1}{2\pi}\left(c_1\frac{\omega_j}{\omega_1} + c_2\sqrt{\frac{\omega_1}{\omega_j}}\right). \tag{3.8}$$

This model essentially captures the feedback between the heat release rate fluctuations and the acoustic pressure fluctuations. More details of the model can be obtained in Balasubramanian & Sujith (2008). The mathematical model governed by (3.5) and (3.6) represents a nonlinear oscillator which exhibits a transition to the self-sustained oscillatory state through subcritical Hopf bifurcation. This model has been used extensively to study various thermoacoustic phenomena in previous studies (Juniper 2011; Magri & Juniper 2013; Zhao & Reyhanoglu 2014; Thomas *et al.* 2018). All the parameters are chosen in such a way that the model exhibits limit cycle oscillations away from the bistable regime.

Parameter	Value	Parameter	Value	Parameter	Value
N	10	τ	0.2	K	0.72
γ	1.4	M	0.005	x_f	0.25
c_1	0.1	c_2	0.06	ω_j	$j\pi$

TABLE 1. The parametric values used for the computation of Rijke tube model.

To study the effect of external perturbations, a harmonic forcing with amplitude, A_f, and frequency, f_f, is implemented. Once we include the forcing term, equation (3.6) becomes:

$$\frac{\mathrm{d}\dot{\eta}_j}{\mathrm{d}t} + 2\zeta_j\omega_j\dot{\eta}_j + {\omega_j}^2\eta_j = -j\pi K\left[\sqrt{\left|\frac{1}{3}+u_f'(t-\tau)\right|}-\sqrt{\frac{1}{3}}\right]\sin(j\pi x_f) + A_f\sin(2\pi f_f t). \tag{3.9}$$

For the present study, we vary both A_f and f_f independently over a wide range when the system is in the state of limit cycle oscillation and analyse the forced response dynamics of the acoustic pressure (p', following (3.4)) in the system. Further, we evaluate heat release rate oscillations ($\dot{q}'$, following (3.10)) for different forcing conditions to analyse the normalized and cycle-averaged acoustic power production ($\langle p'\dot{q}'\rangle_t$). The parametric values used for computation are given in table 1.

$$\dot{q}' = \sum_{j=1}^{N} j\pi K\left[\sqrt{\left|\frac{1}{3}+u_f'(t-\tau)\right|}-\sqrt{\frac{1}{3}}\right]\sin(j\pi x_f). \tag{3.10}$$

4. Results and discussions

During the experiments, we set the heater location (27 cm from the inlet), heater power (1.24 kW corresponding to 4.1 V and 303 A) and the air flow rate (100 slpm) in such a way that the Rijke tube exhibits limit cycle oscillations in acoustic pressure with a natural frequency (f_{n0}) of 168.8 Hz (fundamental mode of the system). The dynamics of such a system with the variation of the parameters mentioned above has been well studied by various researchers; see for example, Matveev (2003), Gopalakrishnan & Sujith (2014) and Etikyala & Sujith (2017). Here, we consider the system in its self-sustained oscillatory state to explore the forced synchronization behaviour when the frequency and the amplitude of forcing are varied independently.

4.1. *Synchronization map*

The response dynamics of the acoustic pressure oscillation is presented in the form of 1 : 1 (the ratio between the forcing frequency and the natural frequency at the synchronized state) forced synchronization map (figure 2*a*) by varying the forcing amplitude (A_f) and the normalized forcing frequency (f_f/f_{n0}) one at a time. Further, the response dynamics obtained from the model is shown in figure 2(*b*). The different regimes of forced synchronization such as regimes of phase locking, phase trapping and phase drifting (Li & Juniper 2013*c*) are identified and illustrated in figures 2(*a*) and 2(*b*).

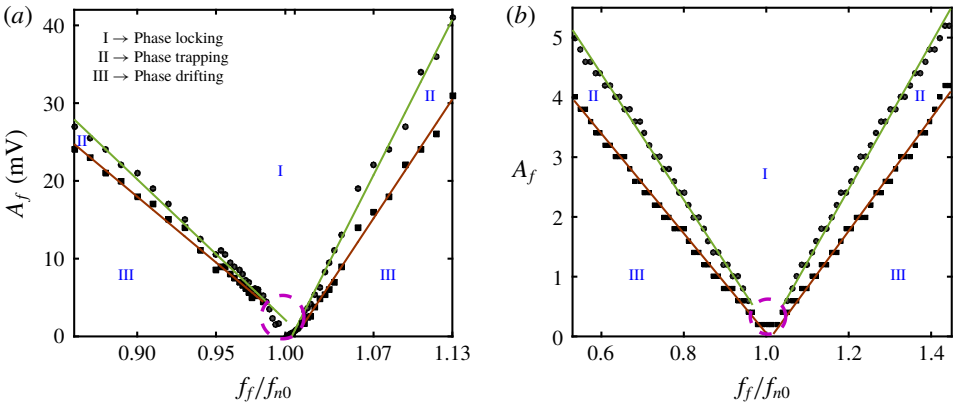

FIGURE 2. (Colour online) A 1:1 forced synchronization map in the plane of A_f and f_f/f_{n0} obtained from (*a*) the experiment and (*b*) the model when a harmonic forcing is applied to a self-sustained thermoacoustic oscillator exhibiting limit cycle oscillations. Regions of phase locking, phase trapping and phase drifting are indicated as regions I, II and III, respectively. The synchronization region indicated by phase locking is observed to form an Arnold tongue. Boundaries between regions I and II (●) and between regions II and III (■) are shown by linearly fitted lines (least squares, $R^2 = 0.99 \pm 0.0044$). The regime where phase trapping is not observed is indicated with a dashed circle. Note that the ranges of abscissa and ordinate in (*a*) and (*b*) are different, where both plots show a qualitative but not a quantitative comparison between the Arnold tongues obtained from experiment and model.

The characterization of the different states of synchronization is based on the dynamics of the instantaneous phase difference ($\Delta\phi$) between the forcing signal (ϕ_F) with the signal of the forced system ($\phi_{p'}$), i.e. $\Delta\phi = |\phi_F - \phi_{p'}|$. The instantaneous phases are calculated through Hilbert transform of the respective signals. During the phase-locking state, the instantaneous phases (ϕ) as well as the frequencies (ω) of the forcing and the response signals show a perfect locking, i.e. $|\Delta\phi| = \text{const.}$ and $\Delta\omega = |\omega_F - \omega_{p'}| = 0$ (Pikovsky *et al.* 2003). In contrast, during the phase trapping state, the relative phase ($\Delta\phi$) between the response signal and the forcing signal shows a bounded oscillatory behaviour, which results in the locking of mean frequencies ($\omega = \langle \mathrm{d}\phi/\mathrm{d}t \rangle$) of the signals without exhibiting their instantaneous phase locking (Thévenin *et al.* 2011; Li & Juniper 2013*c*). Phase drifting, on the other hand, corresponds to the unbounded growth or decay of the unwrapped relative phase between the forcing and the response signals with time.

With an increase in the forcing amplitude, the region of 1 : 1 synchronization increases, resulting in a V-shaped synchronization region (I, figure 2*a*,*b*), called the Arnold tongue (Pikovsky *et al.* 2003; Balanov *et al.* 2009). The model qualitatively captures the phenomenon of 1 : 1 synchronization (figure 2*b*) observed in the experiments (figure 2*a*). We notice a region of phase trapping (II, figure 2*a*,*b*) between the regions of phase drifting (III, figure 2*a*,*b*) and phase locking (I, figure 2*a*,*b*) for both $f_f/f_{n0} < 1$ and $f_f/f_{n0} > 1$.

In the Arnold tongue obtained from experiments (figure 2*a*), we observe an asymmetry about f_{n0}. The curves are less steep for $f_f < f_{n0}$ as compared to that observed for $f_f > f_{n0}$. Such an asymmetry in the Arnold tongue is due to the nonlinearity involved in the periodic oscillator (Balanov *et al.* 2009). A similar

asymmetry in the Arnold tongue has been observed in forced low density jets (Hallberg & Strykowski 2008) and hydrodynamically self-excited jets (Li & Juniper 2013*a*,*c*). However, in another study on a jet diffusion flame, the asymmetry showed the opposite trend, having steeper curves for $f_f < f_{n0}$ (Li & Juniper 2013*b*). We further observe a small region in the parameter space where phase drifting directly transitions to phase locking without phase trapping when the forcing frequency is very close to the f_{n0} (shown as a dashed circle in figure 2*a*,*b*), corresponding to the mechanism of phase locking (here we refer to the route and not the state) towards forced synchronization (Balanov *et al.* 2009). Whereas, the state of phase trapping is exhibited between phase drifting and phase locking in the regime corresponding to the mechanism of suppression.

Having described the overall synchronization behaviour of a forced Rijke tube oscillator, let us look at the transition in the forced dynamics and synchronization state as we vary the forcing parameters individually.

4.2. *Synchronization states achieved as the frequency and amplitude of forcing are varied independently in experiments*

4.2.1. *Effect of the variation of forcing frequency*

First, we vary the forcing frequency (f_f = 90 Hz–220 Hz) across the natural frequency of the system ($f_{n0} = 168.8$ Hz) keeping the forcing amplitude (A_f) fixed at 5 mV. The value of A_f is chosen such that we are able to look into different states of forced synchronization occurring through the mechanism of suppression when f_f is varied. We observe different features of the forced synchronization and the response dynamics of the acoustic pressure. Representative states of synchronization and corresponding forced dynamics are shown for four different values of f_f (figure 3).

The response dynamics of the acoustic pressure signals subjected to harmonic forcing can be inferred from the first return map (figure 3I) and the time series shown in figure 3I (inset). Further, the spectral properties such as frequency of the response signal (figure 3II) and instantaneous relative phase (calculated through Hilbert transform) between forcing and response signals are shown in figure 3II (inset). The forcing frequencies are indicated by red dots in the amplitude spectra (figure 3II).

When f_f is 90 Hz (far from f_{n0}, figure 3*a*II), the dynamics of the response signal is insensitive to forcing (inset of figure 3*a*I). The relative phase shows a continuous drift with time (inset of figure 3*a*II), indicating that the forcing and the response oscillations are desynchronized.

When the value of f_f (= 161.5 Hz) is close to f_{n0} (figure 3*b*II), the amplitude of the response signal shows modulation, known as beats (inset of figure 3*b*I) with a beating frequency of $|f_r - f_f|$, where f_r is the response frequency. First return map of such modulated oscillations shows an oval shaped loop around the diagonal line, indicating two frequency oscillation. On the other hand, a staircase-like structure in the dynamics of the relative phase (inset of figure 3*b*II) indicates a state of intermittent phase locking, where the spans of the phase locked states are separated by jumps (also referred to as phase slips) of integer multiples of 2π radians.

When f_f (= 164.3 Hz) is very near to f_{n0}, however, outside the phase-locking boundary (figure 3*c*II), the relative phase indicates the presence of a phase trapping state, as inferred from the bounded and oscillatory behaviour of the relative phase. Such an oscillatory relative phase has a frequency equal to the beating frequency of the response signal (inset of figure 3*c*II). Although the mean frequencies ($\omega = \langle \mathrm{d}\phi/\mathrm{d}t \rangle$)

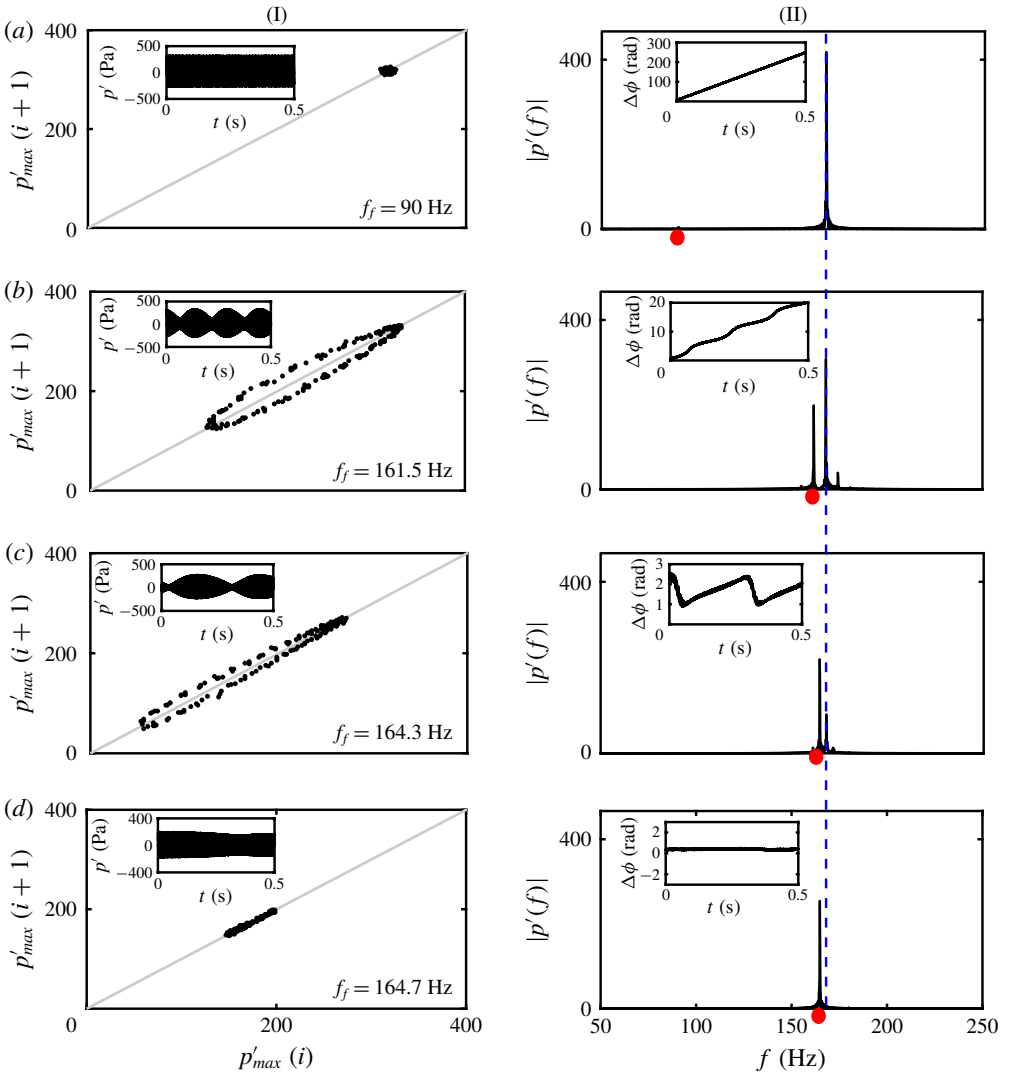

FIGURE 3. (Colour online) As f_f is varied towards f_{n0} (168.8 Hz), we observe different dynamical states in the response signal (I) and different states of synchronization (II, inset) such as phase drifting (a, $f_f = 90$ Hz), intermittent phase locking (b, $f_f = 161.5$ Hz), phase trapping (c, $f_f = 164.3$ Hz) and phase locking (d, $f_f = 164.7$ Hz). Dynamics is presented by plotting the return map (I) and the corresponding time series (inset of I). Amplitude spectrum (forcing frequency is indicated by red dots) of the response signals (II) along with the relative phase dynamics (inset of II) are shown to identify the state of synchronization. The response frequency (f_r) corresponding to natural oscillations is marked with a dashed line in the amplitude spectra.

of the forcing and the response signals are perfectly locked, the amplitude spectrum of the response signal still shows two distinct frequency peaks corresponding to f_f and f_r. This reflects in the beating structure of the response signal (inset of figure 3*c*I), and a closed-loop structure along the diagonal line in the first return map (figure 3*c*I).

During the onset of phase-locking state ($f_f = 164.7$ Hz), the frequency peak corresponding to f_r gets completely suppressed, thus showing a single peak at the

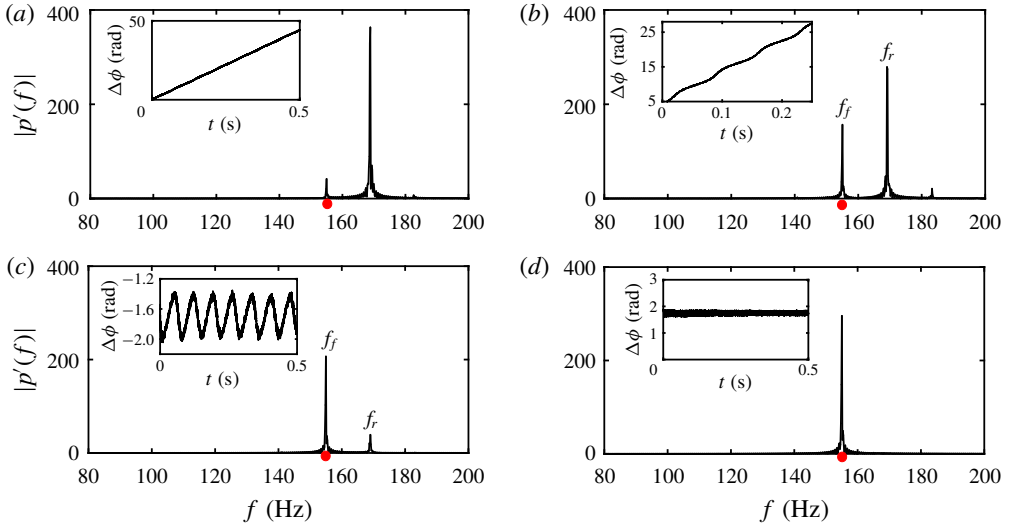

FIGURE 4. (Colour online) The plots show frequency spectra of the response signal, and temporal variation of the relative phase between the response dynamics and the forcing signal (insets) at different values of (*a*) $A_f = 3$ mV, (*b*) $A_f = 12$ mV, (*c*) $A_f = 18$ mV and (*d*) $A_f = 24$ mV, when f_f is maintained constant at 155 Hz, which is sufficiently away from f_{n0} (168.8 Hz). The red dot in the frequency spectra corresponds to the location of the forcing frequency (f_f).

forcing frequency (figure 3*d*II). During this state, the relative phase fluctuates around a constant phase shift (inset of figure 3*d*II) indicating a perfect locking of the instantaneous phases. The first return map corresponding to this state, hence, shows a cluster of points congregated along the diagonal line (figure 3*d*I).

When f_f is varied in such a way that it crosses the right boundary of the synchronization region (see Arnold tongue in figure 2), the observations of forced synchronization states such as phase trapping, intermittent phase locking and phase drifting are repeated in the response dynamics (not shown here for brevity).

4.2.2. *Effect of the variation of forcing amplitude*

We further investigate the effect of forcing amplitude on the response dynamics. Towards that purpose, we vary the forcing amplitude, maintaining the forcing frequency constant at $f_f = 155$ Hz (significantly away from f_{n0}, chosen to look into different states of forced synchronization occurring through the mechanism of suppression, as shown in figure 4) and at $f_f = 167.5$ Hz (very close to f_{n0}, chosen to look into different states of forced synchronization occurring through the mechanism of phase locking, as shown in figure 5).

For $f_f = 155$ Hz, when the amplitude of forcing is very small ($A_f = 3$ mV), the external forcing does not affect the natural oscillations, resulting in a behaviour of phase drifting between the forcing and the response signals (inset of figure 4*a*). With the increase of forcing amplitude to 12 mV, we observe a beating phenomenon (not shown here) in the amplitude of the response signal. This corresponds to a state of intermittent phase locking, confirmed from the observation of a wavy staircase-like structure in the relative phase dynamics (inset of figure 4*b*). As we further increase A_f ($A_f = 18$ mV), we notice a shift in dominance of the peak frequencies from f_r

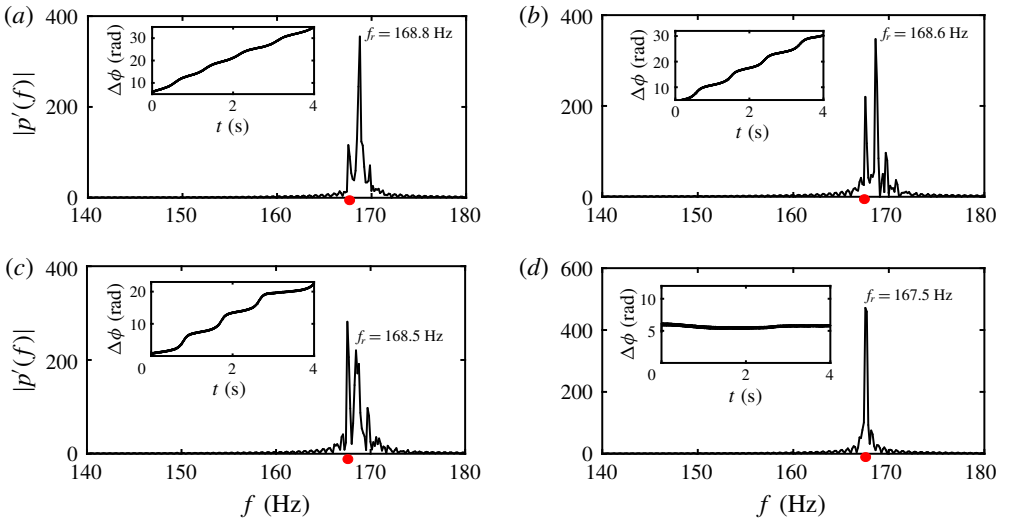

FIGURE 5. (Colour online) Plots showing amplitude spectra of the response signal, and instantaneous relative phase variation between the response and the forcing signal (insets), obtained for different values of $A_f = 0.4$ mV (*a*), 0.8 mV (*b*), 1.2 mV (*c*) and 1.7 mV (*d*), when f_f (167.5 Hz) is very close to f_{n0} (168.8 Hz).

to f_f in the amplitude spectrum (see figure 4*c*). This results in the bounded nature of the relative phase, where the phase difference between the forcing and the response signals is trapped between finite values and oscillates in a periodic manner (inset of figure 4*c*). When the forcing amplitude is sufficiently high ($A_f = 24$ mV), we observe a perfect locking of instantaneous phases of the signals (inset of figure 4*d*), wherein the natural oscillations get completely suppressed and the system oscillates with the forcing frequency (figure 4*d*). Therefore, at $f_f = 155$ Hz, forced synchronization occurs through the mechanism of suppression of natural oscillation (Balanov *et al.* 2009).

For $f_f = 167.5$ Hz, when A_f is very small (0.4 mV, figure 5*a*), the plot of relative phase shows a phase drifting behaviour, which subsequently transitions to a staircase-like structure at a higher value of the forcing amplitude ($A_f = 0.8$ mV in figure 5*b*). When $A_f = 1.2$ mV, we notice a shift in the response frequency (f_r) towards the forcing frequency (f_f) as shown in figure 5(*c*). We, further, observe an intermittent phase-locking behaviour in the dynamics of the relative phase (inset of figure 5*c*). When the amplitude of forcing is high ($A_f = 1.7$ mV), the natural frequency eventually gets locked with the forcing frequency (inset of figure 5*d*). Here, we notice that the transition from phase drifting to phase locking does not happen through phase trapping. The region of the Arnold tongue for which the state of phase trapping does not appear at the synchronization boundary (shown with a dashed circle in figure 2) is referred to as a phase locking region as forced synchronization occurs through the mechanism of phase locking in this region. The mechanisms of phase locking and suppression correspond to saddle-node and torus-death bifurcation, respectively (Balanov *et al.* 2009). In the present study, we report the experimental observation of both the routes in a Rijke tube. Having characterized the different forced dynamics and synchronization behaviour, we now shift our attention to understand the effect of harmonic forcing on the amplitude of the response signal.

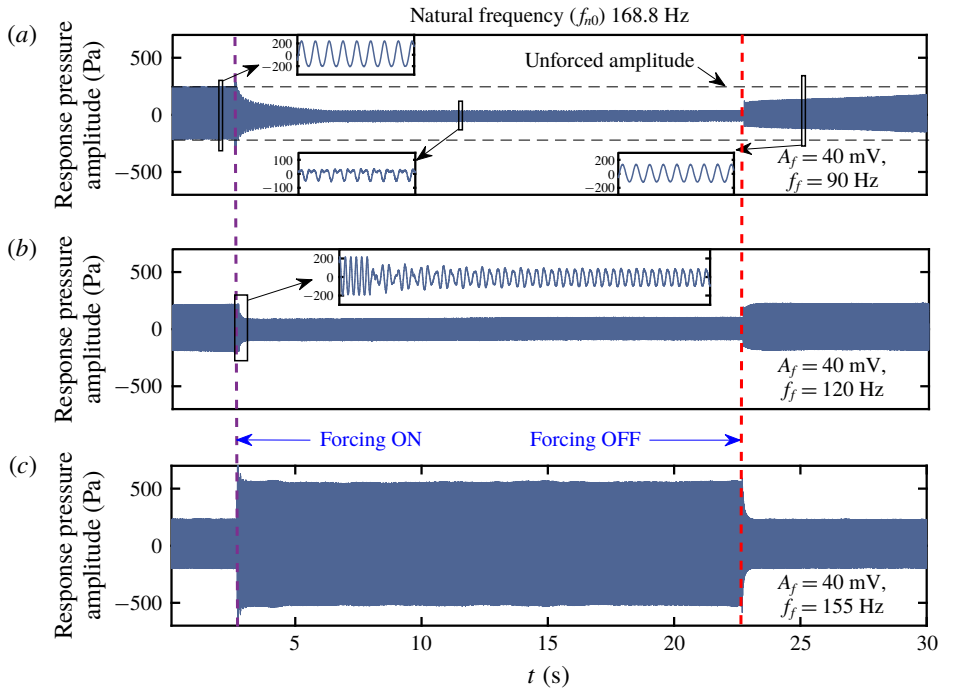

FIGURE 6. (Colour online) The time series of the acoustic pressure oscillations obtained from experiments showing the effect of forcing on the amplitude of the response signal for (*a*) $f_f = 90$ Hz, (*b*) $f_f = 120$ Hz and (*c*) $f_f = 155$ Hz, keeping the forcing amplitude fixed at 40 mV. Depending upon the forcing frequency, the response oscillations can be quenched or amplified.

4.3. *Effect of harmonic forcing on response amplitude*

The overall amplitude of the forced system is referred to as the response amplitude from here on for brevity. Depending upon the choice of forcing parameters (i.e. f_f and A_f), the amplitude response of the system could be different. Typical time series of the acoustic pressure oscillations obtained in experiments for different values of forcing frequency are shown in figure 6. The time instances when the forcing is switched on and off are marked with violet and red dashed lines, respectively. The unforced pressure oscillation in the Rijke tube is periodic (see inset of figure 6*a*) with an amplitude of nearly 215 Pa and a natural frequency of 168.8 Hz.

We vary f_f starting from 90 Hz towards the natural frequency (168.6 Hz) keeping the forcing amplitude constant (40 mV). We find both reduction and increase in the response amplitude of forced oscillation depending upon the frequency of forcing. The acoustic pressure oscillations at forcing frequencies of 90, 120 and 155 Hz are shown in figure 6. When we force the system with a forcing frequency around 90 Hz, we find a maximum reduction in the response amplitude where the dynamics of the forced system does not exhibit sinusoidal oscillations (see inset of figure 6*a*), indicating the existence of nonlinear interaction between the forced and the natural oscillations. We further note that the epoch of the initial transient in the signal after the forcing is switched on is long, i.e. around 5 s at $f_f = 90$ Hz. Once the forcing is switched off, the system takes an even longer time to get back to the original unforced state of oscillation. At this forcing frequency, the thermoacoustic oscillations get destabilized

due to the disturbance induced by the external forcing (the analysis is given in § 4.7). Therefore, once the forcing is switched off, the re-establishment of thermoacoustic oscillations takes a long time.

We find a reduction in the response amplitude even when $f_f = 120$ Hz (figure 6*b*). However, the reduction in amplitude is less compared to the previous case. Therefore, we believe that a low frequency forcing seems to be beneficial for mitigating thermoacoustic instability in practical systems to the extent that the system behaves like a periodic oscillator with a single dominant frequency. However, an experimental validation on more complicated thermoacoustic systems with many degrees of freedom needs to be performed. We further observe that the transient is short compared to the previous case and is aperiodic in nature (inset of figure 6*b*). On the other hand, the forcing with a frequency ($f_f = 155$ Hz) close to the natural frequency ($f_{n0} = 168.8$ Hz) of the system leads to an amplification of the response signal (figure 6*c*). This suggests that choosing a forcing frequency close to the natural frequency for controlling the thermoacoustic instabilities can be even more dangerous for the life of the systems.

Therefore, from a practical point of view, it is important to explore the effect of harmonic forcing on the response signal. The phenomena of reduction and amplification of the response signal can be understood with a careful analysis of the forcing and the self-excited oscillation separately.

4.4. *Effect of harmonic excitation on the amplitudes of self-excited and forcing oscillations*

We further analyse the effect of harmonic excitation on the amplitudes of the self-excited and the forcing oscillations separately. To that end, we obtain amplitudes of the self-excited oscillation (A_n corresponding to the response frequency, f_r) and that of the forcing (A_f corresponding to the forcing frequency, f_f) from the amplitude spectrum (by fast Fourier transform) of the response pressure signal. The normalized amplitudes (A_n/A_0 and A_f/A_0) are plotted with the normalized forcing frequency (f_f/f_{n0}), where A_0 is the unforced spectral amplitude of the self-excited oscillations from both experimental data and model (figure 7). For this plot, the forcing frequency is varied, keeping the forcing amplitude constant (5 mV in experiment and 0.35 in model). We further plot the r.m.s. value of pressure oscillations obtained from experiments (figure 7*a*) and from the model (figure 7*a*) as we vary f_f. We observe an asymmetry across the natural frequency in the amplitude response plots of the forced limit cycle oscillations. We further notice two distinct phenomena occurring simultaneously while f_f/f_{n0} is close to 1.

The amplitude corresponding to the self-excited oscillations (A_n/A_0) shows a gradual decrease as f_f/f_{n0} approaches 1. Such reduction in the amplitude of self-excited oscillations occurs due to the phenomenon of synchronous quenching until the onset of phase locking is observed (figures 7*a* and 7*b*, represented in red squares). In the regime of frequency or phase locking of the Arnold tongue (shown in figure 2), the spectral amplitude of self-excited oscillations is completely suppressed. In the same regime of frequency ratio, the amplitude of forced oscillation (A_f/A_0) initially shows a gradual increase as f_f/f_{n0} approaches 1 (figures 7*a* and 7*b*, represented in blue circles) and then exhibits a sudden jump to a very large amplitude at the onset of phase locking due to the effect of resonance amplification (Odajima *et al.* 1974; Ohe & Takeda 1974; Abel *et al.* 2009). Thus, the simultaneous occurrence of synchronous quenching of natural oscillations and resonance amplification of the

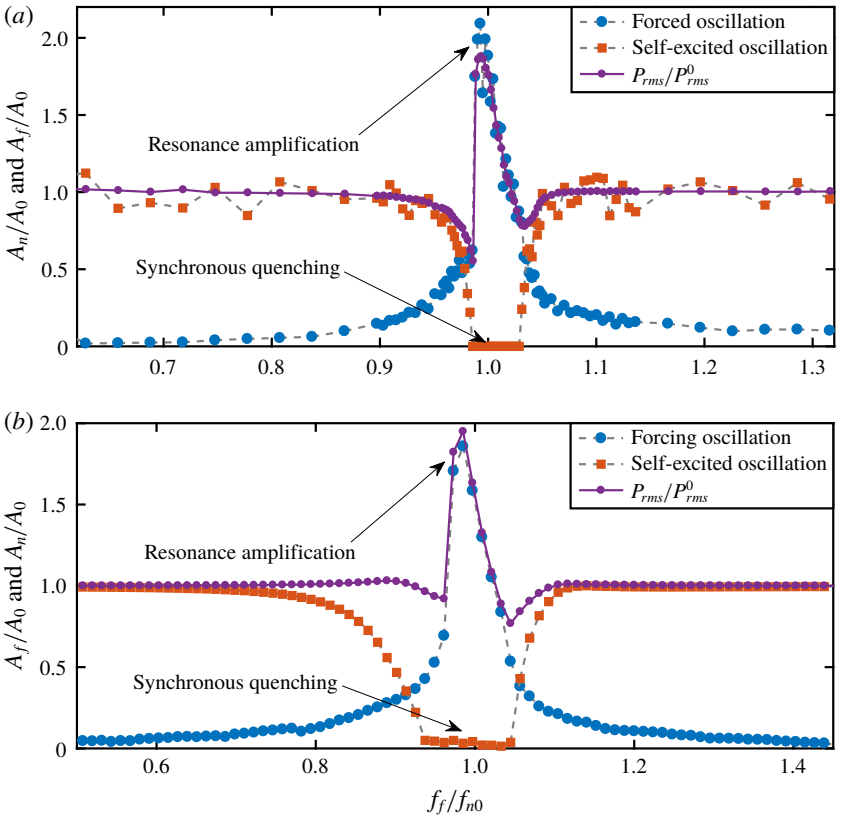

FIGURE 7. (Colour online) Variation of spectral amplitude of self-excited oscillation (A_n/A_0, in red squares) and of forcing (A_f/A_0, in blue circles) when the forcing frequency is varied across the natural frequency of the Rijke tube at a constant value of forcing amplitude ($A_f = 5$ mV in experiment and, $A_f = 0.35$ in model), obtained from experiment (a) and model (b). Synchronous quenching of self-excited oscillations occurs when the forcing frequency (f_f) is close to the natural frequency. This is associated with resonance amplification of the forcing signal. Due to the combined effects of synchronous quenching of the natural oscillation and resonant amplification of the forcing, there is an overall amplification in the P_{rms}/P^0_{rms} value of the response signal (a,b) where P^0_{rms} is the r.m.s. value of unforced pressure oscillation.

forcing signal makes the response signal dominated by the forcing signal. This, in turn, results in the phase locking between the forcing and the response signals. Further, due to the combined effects of synchronous quenching of natural oscillations and resonant amplification of forcing, the r.m.s. value of the response pressure oscillation shoots up to a very high value, compared to the unforced amplitude of the signal, in the synchronization region and then exhibits a gradual decrease with the further increase in f_f/f_{n0} (violet curve in figure 7a). We call this shooting up of the response amplitude (around $f_f = f_{n0}$) synchronance (synchronization–resonance). Such simultaneous occurrence of synchronization and resonance in the frequency locking region has also been reported by Abel *et al.* (2009) who conducted experiments with a self-excited organ tube forced externally using a loudspeaker. Further, we notice that when the value of forcing frequency is far away from f_{n0}, the amplitude of

natural oscillations is not affected by the forcing, and thereby, the r.m.s. value of the response signal is also unaltered.

4.5. *Effect of forcing on the response amplitude*

We further examine the r.m.s. value of response pressure oscillation when A_f is varied keeping f_f fixed at different values. Four values of f_f are chosen in such a manner that two of them are close to f_{n0} and the other two are relatively further away from f_{n0}. We observe that the response amplitude of the acoustic pressure first decreases to a minimum value prior to exhibiting a linear increase, which is primarily due to the gradual increase in the forcing amplitude. This behaviour is observed for $f_f < f_{n0}$ (figure 8*a*,*b*) and also for $f_f > f_{n0}$ only when the frequency detuning is small (figure 8*c*). This reduction in the amplitude of the acoustic pressure signal is not observed when f_f is significantly larger than f_{n0} (figure 8*d*), wherein the response amplitude shows a continuously increasing trend without any minima. From the analysis of relative phase between the forcing and the forced oscillations, as shown in figures 4 and 5, we notice that the minimum in the plot of response amplitude (see figure 8) is close to the boundary of the phase-locking regime (shown as the shaded portion in figure 8*a–c*). In the region of perfect phase locking, the response amplitude of the acoustic pressure oscillations demonstrates almost a linear growth with an increase in A_f. Such a growth of the response amplitude of pressure signal in the synchronization region is significantly steep when f_f is close to f_{n0} (figure 8*b*,*c*). This rapid amplification of the r.m.s. values of response pressure oscillations when f_f/f_{n0} approaches 1 happens due to the phenomenon of synchronance as explained earlier in figure 7. However, the growth in the response amplitude of the pressure signal in the synchronization region is moderate when f_f is much lower than f_{n0} (figure 8*a*). We further notice that the minimum value of the response amplitude, observed prior to the onset of perfect phase-locking state, increases as f_f is increased.

4.6. *Characterization of maximum reduction in the response amplitude due to harmonic forcing*

The reduction in the r.m.s. value of the response pressure signal due to harmonic forcing is shown in figure 9 when we vary f_f across f_{n0}, and for each value of f_f we further vary A_f to obtain the minimum amplitude for that particular f_f. Suppression $(P_0 - P_{min})$ in the amplitude of the response signal is normalized with the r.m.s. value of the unforced natural oscillation (P_0), where P_{min} represents the minimum r.m.s. value of the response signal achieved while A_f is varied for each value of f_f. We observe the maximum reduction in the amplitude of the response signal when f_f is significantly lower than the natural frequency (f_{n0}). As we move towards f_{n0}, the amount of amplitude reduction gradually decreases (figure 9*a*). This also suggests that the effectiveness of forcing in suppressing the amplitude of the unforced oscillation decreases as f_f approaches f_{n0}.

We do not observe any reduction in the response amplitude when $f_f > f_{n0}$ in experiments (figure 9*a*). In other words, when $f_f > f_{n0}$, the r.m.s. value of the response signal does not reduce at all as A_f is varied (see figure 8*d*). Similar observation has been mentioned in Lubarsky *et al.* (2003), Bellows *et al.* (2008) and Abel *et al.* (2009). Amplification of the forcing signal has been found in a system of self-excited organ pipe for $f_f > f_{n0}$ (Abel *et al.* 2009) and in a laminar flame combustor for $f_f < f_{n0}$ as well as $f_f > f_{n0}$ (Guan *et al.* 2018). Thus, forcing the limit cycle oscillation at a frequency greater than the natural frequency of the oscillations might not lead to a

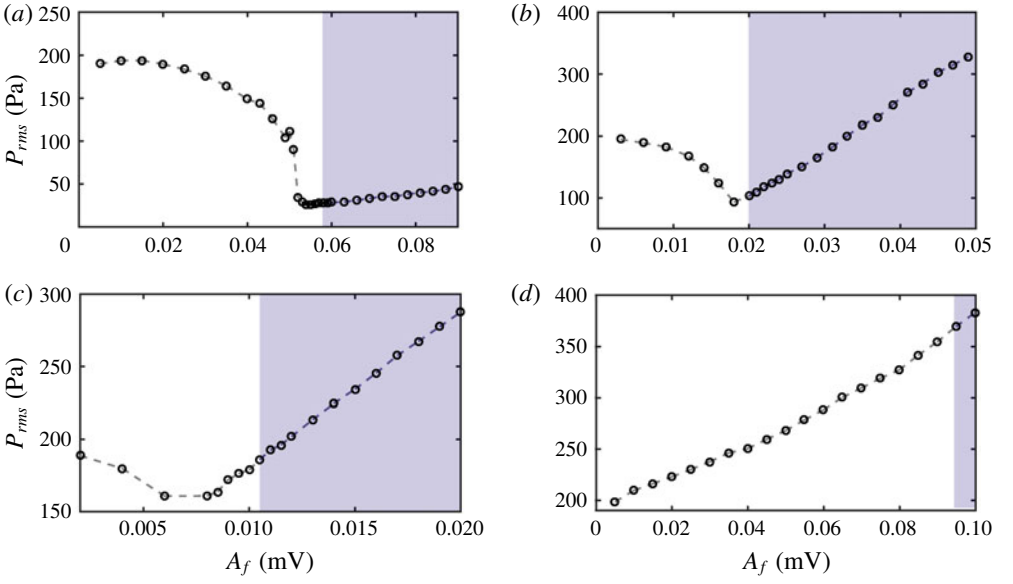

FIGURE 8. (Colour online) The variation of response amplitude (P_{rms}) of the acoustic pressure signals obtained from experiments as A_f is varied for different $f_f = 100$ Hz (*a*), 155 Hz (*b*), 175 Hz (*c*) and 200 Hz (*d*). Reduction in response amplitude is observed for all forcing frequencies except when f_f is sufficiently higher than f_{n0} (*d*). The shaded region indicates the zone of phase locking.

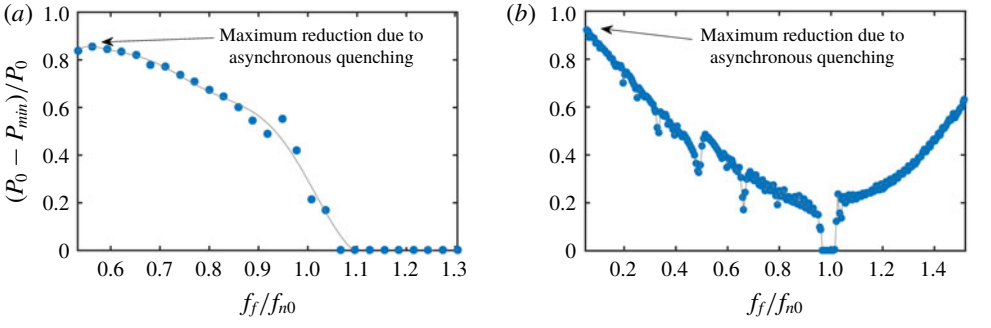

FIGURE 9. (Colour online) Amplitude reduction as a function of normalized forcing frequency (f_f/f_{n0}) obtained from experiments (*a*) and model (*b*) representing the maximum decrease in overall response amplitude of the acoustic pressure signal when f_f is varied across f_{n0}. The amplitude reduction ($P_0 - P_{min}$) is normalized with the r.m.s. value of the unforced amplitude (P_0), where P_{min} represents the minimum r.m.s. value achieved while A_f is varied for a particular value of f_f.

significant suppression of the overall amplitude of the limit cycle, depending on the thermoacoustic system involved.

When f_f/f_{n0} is around 0.6, i.e. the forcing frequency is near the subharmonic frequency of natural oscillations ($f_{n0}/2$), the reduction in response amplitude of the limit cycle oscillations in the system reaches almost 80 % of their unforced amplitude (figure 9*a*). Such a suppression in natural oscillation that occurs when f_f

is significantly away from f_{n0} is due to the phenomenon of asynchronous quenching (Minorsky 1967; Staubli 1987). During asynchronous quenching, we notice that the minimum amplitude achieved through forcing is close to that of the imposed forcing amplitude. Therefore, we suggest that the occurrence of asynchronous quenching through the proper choice of forcing parameters can be effective in mitigating the amplitude of thermoacoustic instability while forced at a frequency much lower than the natural frequency.

On performing a similar analysis in the model, we observe a reduction in the response amplitude of as high as 95 % of the unforced amplitude when f_f/f_{n0} is $\sim$0.03 (figure 9*a*). Therefore, the model chosen in this study is able to capture the phenomenon of amplitude reduction due to asynchronous quenching qualitatively, but not quantitatively. Further, the amplitude reduction of the response signal is found even when the system is forced with $f_f > f_{n0}$ (figure 9*b*). The phenomenon of asynchronous quenching occurring at both $f_f/f_{n0} < 1$ and $f_f/f_{n0} > 1$ is not observed in the present experimental set-up. However, using a laminar flame combustor, Guan *et al.* (2018) showed the existence of asynchronous quenching for $f_f < f_{n0}$ as well as $f_f > f_{n0}$, which qualitatively corroborates the forced Duffing–van der Pol oscillator with weak nonlinearity.

4.7. *Physical explanation for the amplitude suppression due to asynchronous quenching*

As the phenomenon of thermoacoustic instability is a consequence of positive coupling between the acoustic pressure (p') and the heat release rate ($\dot{q}'$) oscillations, it is critical to explore the effect for harmonic forcing on such thermoacoustic coupling. As we do not have a means to measure $\dot{q}'$ (3.10) in the present experimental facility of the Rijke tube, we try to find a plausible explanation from the model that governs the essential features of this system.

The phenomena of synchronous quenching and asynchronous quenching are well captured in the present model of the Rijke tube (refer to figures 7*b* and 9*b*, respectively). Further, the association of resonance amplification of the forcing signal with the synchronous quenching of self-excited oscillations is also well predicted in the model (figure 7*b*). Therefore, in the model, we look into the normalized and cycle-averaged acoustic power production, $\langle p'\dot{q}'\rangle_t$ (where $t = 512 \times$ time period), which is responsible for the sustenance of thermoacoustic instability (Lieuwen & Yang 2005).

The variation of $\langle p'\dot{q}'\rangle_t$ with A_f is shown in figure 10. Here, we choose a forcing frequency ($f_f/f_{n0} = 0.06$) at which the model shows significant reduction in the r.m.s. value of the pressure oscillations (figure 9*b*). With an increase in A_f, $\langle p'\dot{q}'\rangle_t$ decreases (figure 10) and becomes minimum when we achieve maximum reduction in the amplitude of pressure oscillation. The low value of acoustic driving ($\langle p'\dot{q}'\rangle_t$) explains the reduction in the amplitude of self-excited oscillation observed during thermoacoustic instability. Further, we observe that, at the instant of no amplitude reduction, the acoustic pressure and the heat release rate oscillate at the natural frequency (figure 10i) and their relative phase oscillates within 0 and $\pi/2$ rad (figure 10ii), satisfying the Rayleigh criterion (Rayleigh 1878). On the other hand, at the instant of maximum amplitude reduction, both the acoustic pressure and the heat release rate oscillations have a dominant peak at the forcing frequency (figure 10iii), and therefore, they are phase locked, which can be inferred from the bounded relative phase shown in figure 10(iv). Interestingly, at this condition of forcing, the relative

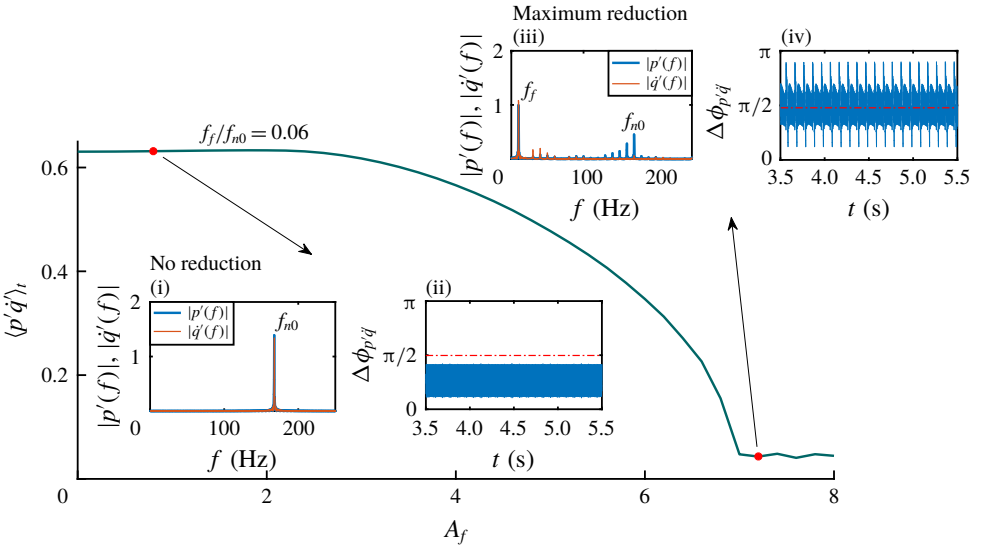

FIGURE 10. (Colour online) Cycle-averaged value of the acoustic power production ($\langle p'\dot{q}'\rangle_t$; $t = 512 \times$ time period) is plotted for a low forcing frequency ($f_f/f_{n0} = 0.06$) and by varying the amplitude of forcing (A_f) in the model. Both p' and $\dot{q}'$ are normalized to zero mean and unit variance, and their product is averaged over 512 cycles. Amplitude spectra of p' and $\dot{q}'$ and the relative phase between them are shown for two different A_f (indicated as red dots) corresponding to the instants of 'no reduction' and 'maximum reduction'.

phase between p' and $\dot{q}'$ oscillates around $\pi/2$ rad, which according to the Rayleigh criterion will lead to an alternative acoustic driving and damping (figure 10iv). This, in turn, is manifested as a very low value ($= 0.045$) of $\langle p'\dot{q}'\rangle_t$ (corresponding to an average phase difference, $\langle \Delta\phi_{p'\dot{q}'}\rangle_t$, of 0.49π) compared to the value (0.63) of $\langle p'\dot{q}'\rangle_t$ during thermoacoustic instability (figure 10). This observation suggests a plausible physical mechanism behind the quenching of thermoacoustic instabilities due to forcing, which mainly happens due the destruction of the positive interaction between p' and $\dot{q}'$ when a high amplitude forcing is applied at the low value of frequency. In summary, asynchronous quenching, which is a characteristic phenomenon of a harmonically forced limit cycle oscillator, appears promising in practical and more complex thermoacoustic systems to suppress the unwanted high amplitude pressure oscillations.

5. Conclusions

We perform both theoretical and experimental investigation of forced synchronization in a simple thermoacoustic system, the horizontal Rijke tube. By varying the forcing frequency and the forcing amplitude, we observe the phenomenon of 1 : 1 synchronization both in the experiments and the model. We further identify different states of synchronization between the response signal and the forcing signal when the forcing amplitude and the forcing frequency are individually varied. When the system is forced with a frequency which is close to its natural frequency, the concurrence of both synchronous quenching of natural oscillations and resonance amplification of the forcing signal is observed along with different states of forced synchronization.

On the other hand, as the forcing frequency (f_f) is fairly lower than the natural frequency (f_{n0}) of the system, a substantial amount of amplitude reduction (almost 80 % of the unforced amplitude in experiments) occurs due to the phenomenon of asynchronous quenching. Such phenomena are usually disregarded by ascribing the dynamics to the 'nonlinear interaction' between the forcing and the self-sustained oscillations without going into details. This is the first study to recognize the maximum reduction in the amplitude is due to the occurrence of asynchronous quenching. We found that asynchronous quenching is associated with the breaking of positive coupling between the acoustic pressure and the heat release rate oscillations in the thermoacoustic system when forced at frequencies considerably lower than their natural frequency of oscillation. The phenomenon of asynchronous quenching found its applications in ion-sound instability (Keen & Fletcher 1969) and self-excited ionization waves (Ohe & Takeda 1974). Quenching of oscillation amplitude in practical thermoacoustic systems such as gas turbine engines is desirable and the occurrence of asynchronous quenching can be helpful for such systems. However, the experimental validity of asynchronous quenching for more complicated thermoacoustic systems (for example, turbulent combustors) with many degrees of freedom needs further investigation. Furthermore, similar characteristics of quenching may be expected in other hydrodynamically self-sustained oscillations as well.

Acknowledgements

The lead author gratefully acknowledges the Institute Post-doctoral Fellowship of the Indian Institute of Technology Madras, India. This work was supported by the Office of Naval Research Global (contract monitor: Dr R. Kolar; grant no. N62909-18-1-2061). The authors also acknowledge the help of Thilagraj for drawing the schematic of the experimental set-up.

REFERENCES

ABEL, M., AHNERT, K. & BERGWEILER, S. 2009 Synchronization of sound sources. *Phys. Rev. Lett.* **103** (11), 114301.

ANISHCHENKO, V. S., VADIVASOVA, T. E., POSTNOV, D. E. & SAFONOVA, M. A. 1992 Synchronization of chaos. *Intl J. Bifurcation Chaos* **2** (03), 633–644.

BALANOV, A., JANSON, N., POSTNOV, D. & SOSNOVTSEVA, O. 2009 Synchronization. In *Springer Series in Synergetics*. Springer.

BALASUBRAMANIAN, K. & SUJITH, R. I. 2008 Thermoacoustic instability in a Rijke tube: non-normality and nonlinearity. *Phys. Fluids* **20** (4), 044103.

BALUSAMY, S., LI, L. K. B., HAN, Z. & HOCHGREB, S. 2017 Extracting flame describing functions in the presence of self-excited thermoacoustic oscillations. *Proc. Combust. Inst.* **36** (3), 3851–3861.

BALUSAMY, S., LI, L. K. B., HAN, Z., JUNIPER, M. P. & HOCHGREB, S. 2015 Nonlinear dynamics of a self-excited thermoacoustic system subjected to acoustic forcing. *Proc. Combust. Inst.* **35** (3), 3229–3236.

BATTOGTOKH, D., AIHARA, K. & TYSON, J. J. 2006 Synchronization of eukaryotic cells by periodic forcing. *Phys. Rev. Lett.* **96** (14), 148102.

BELLOWS, B. D., HREIZ, A. & LIEUWEN, T. 2008 Nonlinear interactions between forced and self-excited acoustic oscillations in premixed combustor. *J. Propul. Power* **24** (3), 628–630.

BELLOWS, B. D., NEUMEIER, Y. & LIEUWEN, T. 2006 Forced response of a swirling, premixed flame to flow disturbances. *J. Propul. Power* **22** (5), 1075–1084.

BLAŽEK, V. 1968 A semiconductor laser as a classical van der Pol oscillator controlled by an external signal. *Czech. J. Phys.* B **18** (5), 644–646.

BOCCALETTI, S., ALLARIA, E., MEUCCI, R. & ARECCHI, F. T. 2002 Experimental characterization of the transition to phase synchronization of chaotic CO_2 laser systems. *Phys. Rev. Lett.* **89** (19), 194101.

CROCCO, L. & CHENG, S.-I. 1956 Theory of combustion instability in liquid propellant rocket motors. *Tech. Rep.* Princeton University NJ.

DINES, P. J. 1984 Active control of flame noise. PhD thesis, University of Cambridge.

DOWLING, A. P. & MORGANS, A. S. 2005 Feedback control of combustion oscillations. *Annu. Rev. Fluid Mech.* **37**, 151–182.

EMERSON, B., O'CONNOR, J., JUNIPER, M. & LIEUWEN, T. 2012 Density ratio effects on reacting bluff-body flow field characteristics. *J. Fluid Mech.* **706**, 219–250.

ETIKYALA, S. & SUJITH, R. I. 2017 Change of criticality in a prototypical thermoacoustic system. *Chaos: Interdiscip. J. Nonlinear Sci.* **27** (2), 023106.

GOPALAKRISHNAN, E. A. & SUJITH, R. I. 2014 Influence of system parameters on the hysteresis characteristics of a horizontal Rijke tube. *Intl J. Spray Combust. Dyn.* **6** (3), 293–316.

GOPALAKRISHNAN, E. A. & SUJITH, R. I. 2015 Effect of external noise on the hysteresis characteristics of a thermoacoustic system. *J. Fluid Mech.* **776**, 334–353.

GREENBLATT, D. & WYGNANSKI, I. J. 2000 The control of flow separation by periodic excitation. *Prog. Aerosp. Sci.* **36** (7), 487–545.

GUAN, Y., GUPTA, V., KASHINATH, K. & LI, L. K. B. 2018 Open-loop control of periodic thermoacoustic oscillations: experiments and low-order modelling in a synchronization framework. In *Proceedings of the Combustion Institute*, Elsevier.

HALLBERG, M. P. & STRYKOWSKI, P. J. 2008 Open-loop control of fully nonlinear self-excited oscillations. *Phys. Fluids* **20** (4), 041703.

HAN, Z., BALUSAMY, S. & HOCHGREB, S. 2015 Spatial analysis on forced heat release response of turbulent stratified flames. *J. Engng Gas Turbines Power* **137** (6), 061504.

HAN, Z. & HOCHGREB, S. 2015 The response of stratified swirling flames to acoustic forcing: experiments and comparison to model. *Proc. Combust. Inst.* **35** (3), 3309–3315.

HECKL, M. A. 1988 Active control of the noise from a Rijke tube. *J. Sound Vib.* **124** (1), 117–133.

HECKL, M. A. 1990 Non-linear acoustic effects in the Rijke tube. *Acta Acust. United Ac.* **72** (1), 63–71.

HUERRE, P. & MONKEWITZ, P. A. 1985 Absolute and convective instabilities in free shear layers. *J. Fluid Mech.* **159**, 151–168.

HUERRE, P. & MONKEWITZ, P. A. 1990 Local and global instabilities in spatially developing flows. *Annu. Rev. Fluid Mech.* **22** (1), 473–537.

HYODO, H. & BIWA, T. 2018 Phase-locking and suppression states observed in forced synchronization of thermoacoustic oscillator. *J. Phys. Soc. Japan* **87** (3), 034402.

JUNIPER, M. P. 2011 Triggering in the horizontal Rijke tube: non-normality, transient growth and bypass transition. *J. Fluid Mech.* **667**, 272–308.

JUNIPER, M. P. & SUJITH, R. I. 2018 Sensitivity and nonlinearity of thermoacoustic oscillations. *Annu. Rev. Fluid Mech.* **50**, 661–689.

KASHINATH, K., LI, L. K. B. & JUNIPER, M. P. 2018 Forced synchronization of periodic and aperiodic thermoacoustic oscillations: lock-in, bifurcations and open-loop control. *J. Fluid Mech.* **838**, 690–714.

KEEN, B. E. & FLETCHER, W. H. W. 1969 Suppression and enhancement of an ion-sound instability by nonlinear resonance effects in a plasma. *Phys. Rev. Lett.* **23** (14), 760.

KIM, K. T. & HOCHGREB, S. 2011 The nonlinear heat release response of stratified lean-premixed flames to acoustic velocity oscillations. *Combust. Flame* **158** (12), 2482–2499.

KIM, K. T. & HOCHGREB, S. 2012 Measurements of triggering and transient growth in a model lean-premixed gas turbine combustor. *Combust. Flame* **159** (3), 1215–1227.

KING, L. V. 1914 On the convection of heat from small cylinders in a stream of fluid: determination of the convection constants of small platinum wires with applications to hot-wire anemometry. *Phil. Trans. R. Soc. Lond.* A **214**, 373–432.

KISS, I. Z. & HUDSON, J. L. 2001 Phase synchronization and suppression of chaos through intermittency in forcing of an electrochemical oscillator. *Phys. Rev.* E **64** (4), 046215.

LANG, W., POINSOT, T., BOURIENNE, F., CANDEL, S. & ESPOSITO, E. 1987*a* Suppression of combustion instabilities by active control. *AIAA Paper* 87-1876.

LANG, W., POINSOT, T. & CANDEL, S. 1987*b* Active control of combustion instability. *Combust. Flame* **70** (3), 281–289.

LI, L. K. B. & JUNIPER, M. P. 2013*a* Lock-in and quasiperiodicity in a forced hydrodynamically self-excited jet. *J. Fluid Mech.* **726**, 624–655.

LI, L. K. B. & JUNIPER, M. P. 2013*b* Lock-in and quasiperiodicity in hydrodynamically self-excited flames: experiments and modelling. *Proc. Combust. Inst.* **34** (1), 947–954.

LI, L. K. B. & JUNIPER, M. P. 2013*c* Phase trapping and slipping in a forced hydrodynamically self-excited jet. *J. Fluid Mech.* **735**, R5.

LIEUWEN, T. C. & YANG, V. 2005 *Combustion Instabilities in Gas Turbine Engines: Operational Experience, Fundamental Mechanisms, and Modeling*. AIAA.

LORES, M. E. & ZINN, B. T. 1973 Nonlinear longitudinal combustion instability in rocket motors. *Combust. Sci. Technol.* **7** (6), 245–256.

LUBARSKY, E., SHCHERBIK, D., ZINN, B., MCMANUS, K., FRIC, T. & SRINIVASAN, S. 2003 Active control of combustion oscillations by non-coherent fuel flow modulation. In *9th AIAA/CEAS Aeroacoustics Conference and Exhibit*, p. 3180. ARC-AIAA.

MAGRI, L. & JUNIPER, M. P. 2013 Sensitivity analysis of a time-delayed thermo-acoustic system via an adjoint-based approach. *J. Fluid Mech.* **719**, 183–202.

MARIAPPAN, S. 2012 Theoretical and experimental investigation of the non-normal nature of thermoacoustic interactions. PhD thesis, Indian Institute of Technology Madras.

MATVEEV, K. I. 2003 Thermoacoustic instabilities in the Rijke tube: experiments and modeling. PhD thesis, California Institute of Technology.

MCMANUS, K. R., VANDSBURGER, U. & BOWMAN, C. T. 1990 Combustor performance enhancement through direct shear layer excitation. *Combust. Flame* **82** (1), 75–92.

MINORSKY, N. 1967 Comments 'On asynchronous quenching'. *IEEE Trans. Autom. Control* **12** (2), 225–227.

MONKEWITZ, P. A. 1988 The absolute and convective nature of instability in two-dimensional wakes at low Reynolds numbers. *Phys. Fluids* **31** (5), 999–1006.

NAJM, H. & GHONIEM, A. 1991 Numerical simulation of the convective instability in a dump combustor. *AIAA J.* **29** (6), 911–919.

NICOUD, F. & WIECZOREK, K. 2009 About the zero Mach number assumption in the calculation of thermoacoustic instabilities. *Intl J. Spray Combust. Dyn.* **1** (1), 67–111.

NOMURA, T., SATO, S., DOI, S., SEGUNDO, J. P. & STIBER, M. D. 1993 A Bonhoeffer–van der Pol oscillator model of locked and non-locked behaviors of living pacemaker neurons. *Biol. Cybernet.* **69** (5–6), 429–437.

ODAJIMA, K., NISHIDA, Y. & HATTA, Y. 1974 Synchronous quenching of drift-wave instability. *Phys. Fluids* **17** (8), 1631–1633.

OHE, K. & TAKEDA, S. 1974 Asynchronous quenching and resonance excitation of ionization waves in positive columns. *Contrib. Plasma Phys.* **14** (2), 55–65.

OHSAWA, T. 1980 Synchronous quenching due to nonlinear mode coupling in beam-plasma system. *J. Phys. Soc. Japan* **49** (6), 2340–2348.

OYEDIRAN, A., DARLING, D. & RADHAKRISHNAN, K. 1995 Review of combustion-acoustics instabilities. In *31st Joint Propulsion Conference and Exhibit*, p. 2469. ARC-AIAA.

PIKOVSKY, A., ROSENBLUM, M. & KURTHS, J. 2003 *Synchronization: A Universal Concept in Nonlinear Sciences*, vol. 12. Cambridge University Press.

VAN DER POL, B. 1920 A theory of the amplitude of free and forced triode vibrations. *Radio Rev.* **1** (1920), 701–710.

PROVANSAL, M., MATHIS, C. & BOYER, L. 1987 Bénard–von Kármán instability: transient and forced regimes. *J. Fluid Mech.* **182**, 1–22.

RAYLEIGH, LORD 1878 The explanation of certain acoustical phenomena. *Roy. Inst. Proc.* **8**, 536–542.

STAUBLI, T. 1987 Entrainment of self-sustained flow oscillations: phaselooking or asynchronous quenching? *J. Appl. Mech.* **54**, 707.

STERLING, J. D. & ZUKOSKI, E. E. 1991 Nonlinear dynamics of laboratory combustor pressure oscillations. *Combust. Sci. Technol.* **77** (4–6), 225–238.

SUJITH, R. I., JUNIPER, M. P. & SCHMID, P. J. 2016 Non-normality and nonlinearity in thermoacoustic instabilities. *Intl J. Spray Combust. Dyn.* **8** (2), 119–146.

THÉVENIN, J., ROMANELLI, M., VALLET, M., BRUNEL, M. & ERNEUX, T. 2011 Resonance assisted synchronization of coupled oscillators: frequency locking without phase locking. *Phys. Rev. Lett.* **107** (10), 104101.

THOMAS, N., MONDAL, S., PAWAR, S. A. & SUJITH, R. I. 2018 Effect of time-delay and dissipative coupling on amplitude death in coupled thermoacoustic oscillators. *Chaos: Interdiscip. J. Nonlinear Sci.* **28** (3), 033119.

VAN DER POL, B. & VAN DER MARK, J. 1928 Lxxii. The heartbeat considered as a relaxation oscillation, and an electrical model of the heart. *Lond. Edinb. Dubl. Phil. Mag. J. Sci.* **6** (38), 763–775.

YOSHIDA, T., YAZAKI, T., UEDA, Y. & BIWA, T. 2013 Forced synchronization of periodic oscillations in a gas column: where is the power source? *J. Phys. Soc. Japan* **82** (10), 103001.

ZHAO, D. & REYHANOGLU, M. 2014 Feedback control of acoustic disturbance transient growth in triggering thermoacoustic instability. *J. Sound Vib.* **333** (16), 3639–3656.